JTTEE5 19:24–30
DOI: 10.1007/s11666-009-9419-x
1059-9630/$19.00 © ASM International

Study of the Splat-Substrate Interface for a NiCr Coating Plasma Sprayed onto Polished Aluminum and Stainless Steel Substrates

S. Brossard, P.R. Munroe, A. Tran, and M.M. Hyland

(Submitted April 5, 2009; in revised form September 14, 2009)

In the plasma spraying process, the mechanisms by which molten particles impact on and bond with the substrate are not fully understood. For this study a nickel-chromium powder was sprayed onto mirror polished aluminum 5052 and stainless steel 304 substrates to form single splats. The splats and their interface with the substrate were studied using detailed microstructural characterization with emphasis on the shape of the splats, the nature of the splat-substrate interface, including the degree of contact and the extent of melting of the substrate and mixing with the splat material, and the presence, either on or within the splats of phases such as oxides. It was shown that melting of the substrate, along with intermixing and diffusion between substrate and splat materials, occurred for the steel substrate, but not for the aluminum substrate. Oxides including nickel oxide, chromium oxide, and aluminum oxide were also observed, the type and distribution of these phases depended on the substrate type.

Keywords aluminum, FIB, NiCr, plasma spray, SEM, stainless steel, TEM

1. Introduction

Thermal spraying processes, and plasma spraying in particular, permit the manufacture of coatings aiming at improving engineering performances and/or increasing component life without affecting the properties of the bulk substrate (Ref 1). The mechanisms of adhesion between the sprayed coating and the substrate have a significant influence on the mechanical properties of the coating. Indeed, Kitahara and Hasui (Ref 2) found that when localized melting of substrate occurs upon impact of the molten particle, an intermetallic layer is usually formed and the bonding is regarded as metallurgical. In such a situation there, authors found that the adhesion strength at the splat-substrate interface was higher than the cohesive strength of the coating and failure tended to occur within the coating itself. If there is no, or only partial, metallurgical bonding, the adhesion strength is much lower. In the absence of substrate melting, adhesion between coating and substrate may occur by mechanical interlocking (especially in case of a substrate with a rough surface) and/or if diffusion occurs at the coating-substrate interface (Ref 3, 4). This requires good contact between splat and substrate, and in that matter splashing of the splat on impact is ideally avoided (Ref 3). Steffens et al. (Ref 4) showed that such contact occurred by diffusive contact zones, which were not present across the entire contact surface of the splat, but only in limited regions separated, usually, by pores at the splat-substrate interface. The degree of contact and interactions at these contact zones were improved by increasing the contact temperature, which, in turn, depended on the properties of both the substrate and splat and the spray conditions.

Interfacial features, including the quality of contact between the splat and substrate, the possible occurrence of melting and the presence of pores and oxides were studied for NiCr particles plasma sprayed onto both stainless steel and aluminum polished substrates. Splat morphology and structure were also characterized. Comparison of the behavior of the two substrates permits an understanding of the role of the nature of the substrate and its properties on splat formation and the interactions of the splat with the substrate. This article is part of a larger study on splat formation for NiCr sprayed on aluminum and steel substrates depending on the surface chemistry, roughness, and spraying method. This article focuses, in particular, on

This article is an invited paper selected from presentations at the 2009 International Thermal Spray Conference and has been expanded from the original presentation. It is simultaneously published in *Expanding Thermal Spray Performance to New Markets and Applications: Proceedings of the 2009 International Thermal Spray Conference*, Las Vegas, Nevada, USA, May 4-7, 2009, Basil R. Marple, Margaret M. Hyland, Yuk-Chiu Lau, Chang-Jiu Li, Rogerio S. Lima, and Ghislain Montavon, Ed., ASM International, Materials Park, OH, 2009.

S. Brossard and **P.R. Munroe**, School of Materials, University of New South Wales, Sydney, NSW 2052, Australia; and **A. Tran** and **M.M. Hyland**, Chemical & Materials Engineering Department, University of Auckland, Auckland 1142, New Zealand. Contact e-mail: sophie.brossard@student.unsw.edu.au.

the influence of the nature of the substrate on the splats' characteristics.

2. Experimental Conditions

Stainless steel 304 and Aluminum 5052 were ground and mirror polished mechanically with diamond paste. The surface average roughness measured by Atomic Force Microscopy was between 5 and 10 nm. Substrates were then plasma sprayed at room temperature with a commercial NiCr alloy powder (Ni80-Cr20, Sulzer Metco 43VF-NF, Wohlen, Switzerland, 5-45 μm), using a Sulzer Metco (Wohlen, Switzerland) 7 MB gun operating at a current of 550 A and a voltage of 74 V. The spraying distance between the gun and the substrate was kept at 80 mm. The powder was injected at a feeding rate of 1 g/min. The plasma gas mixture was nitrogen and hydrogen, to limit to the maximum possible extent the oxidation of the particles during flight. The spray conditions involved a flow rate of 47.6 SLPM (Standard Liters per Minute) and 5.4 SLPM, respectively. Only one pass was made in order to obtain single NiCr splats on the substrate surface.

Characterization of the specimens was carried out using a scanning electron microscope (SEM) (Hitachi S-3400X, Mito, Japan). Measurement of the surface roughness was performed using an atomic force microscope (AFM) (Digital Instrument 3000, Santa Barbara, USA). Cross sections of the splats were prepared using a focused ion beam (FIB) microscope (FEI XP200, Hillsboro, USA). Transmission electron microscope (TEM) cross sections were prepared using a dual beam high resolution focused ion beam instrument (FEI XT Nova Nanolab 200, Hillsboro, USA). They were then lifted out with a micromanipulator and put on a carbon coated copper grid. TEM studies were performed using a Philips CM200 (Eindhoven, The Netherlands) to which an energy dispersive x-ray spectrometer was interfaced.

3. Experimental Results

3.1 Stainless Steel Specimen

SEM images of about 50 single randomly chosen splats were taken and the splat morphology evaluated and the splat diameter, D, measured (features such as splashed fingers were ignored when evaluating diameter, which was done by taking the smallest and largest diameter value measured from the splat, which are not perfectly circular, and calculating the average value). The percentage of each splat type and the median diameter, D_m, are seen to be indicative only, as the number of splats observed is insufficient to establish accurate statistical analysis. A more detailed analysis of splat size has been presented elsewhere (Ref 5). According to their morphology, splats were classified in three categories:

- Disc-shaped splats (~23% of the analyzed series) (Fig. 1a), with, usually, a large central pore (5-10 μm in diameter) which appeared to originate from the release of gas by the substrate upon the impact of the particle. A very slight lip can also often be observed at the splat periphery ($20 < D < 55$ μm, $D_m = 30$ μm).
- Near disc-shaped splats (47% of the analyzed series) (Fig. 1b). A central pore still appears to be present despite the splashy appearance of the splats ($10 < D < 30$ μm, $D_m = 20$ μm).
- Fragmented splats (30% of the analyzed series) (Fig. 1c). Despite the difference in shape with the previous splats, the center of these splats is still NiCr-free ($8 < D < 20$ μm, $D_m = 14$ μm).

For each category of splat, several FIB cross sections were prepared and examined. A typical example for a near disc-shaped splat is shown in Fig. 2. The inset image shows a SEM image of the splat prior to cross-sectioning. In the central pore of the splat (1) can be found a porous oxide phase, which will be shown later by TEM to be mainly NiO, along with some metallic NiCr particles (2). A thin layer of NiCr can be found at the bottom of the pore (3), while the shape of the splat around the central hole shows a distinct rim (4): the NiCr seems to have been ''pushed'' upward on solidification, probably due to the instability of the gas released by the specimen upon impact (4). The large columnar grains (~1-3 μm in size) suggest a slow rate of solidification at the top surface of the splat (4). In certain zones, for example at the interface with the substrate, some small (sub-micron) grains, whose boundaries correspond with the ones of the grains of the splat, are apparent (5). This suggests melting of the substrate has occurred, followed by the simultaneous solidification of both phases. Finally, on the right-hand side of the splat, what seems to be a thin layer of oxide can be

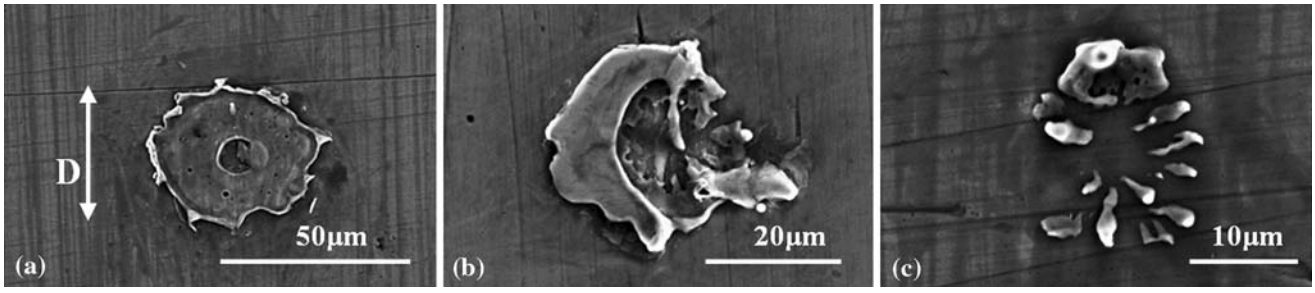

Fig. 1 SEM images of each type of splat found on the stainless steel substrate

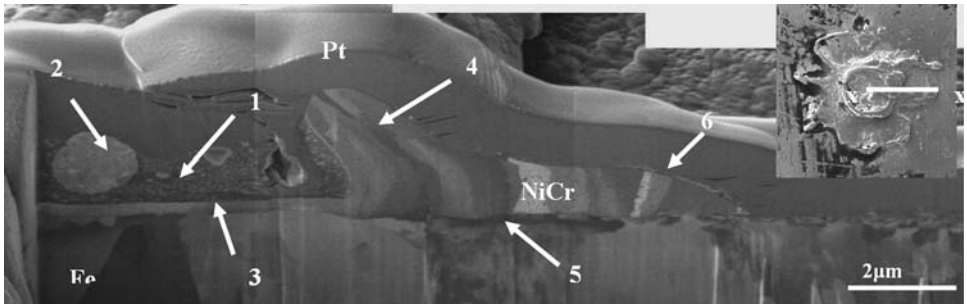

Fig. 2 FIB image of a cross section of a near disc-shaped splat found on the stainless steel substrate

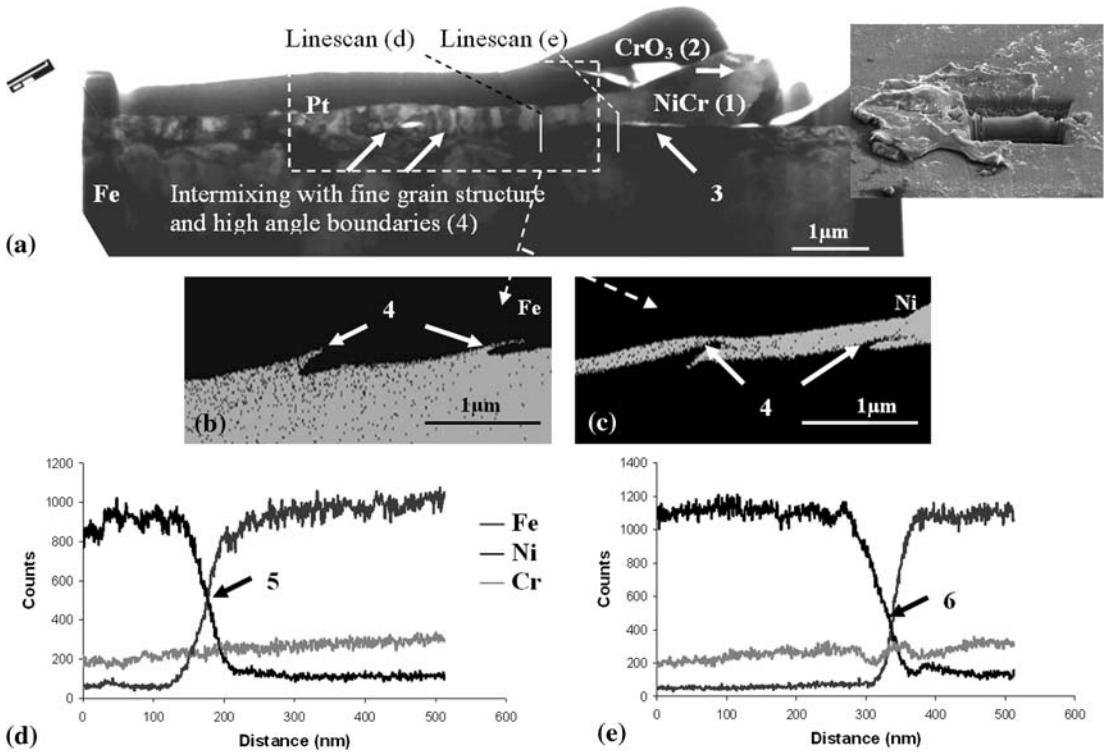

Fig. 3 TEM cross section of a disc-shaped splat from the stainless steel substrate (a) Bright field image, (b, c) EDS elemental maps, (d, e) EDS linescan

observed at the periphery of the splat (6). From the FIB cross sections, the aspect ratio, defined as being the diameter of the splat divided by its thickness, can be calculated. For this splat it has been found to be $\zeta \sim 44$. The thickness is measured on the flat portion of the splat between the central hole and the rim.

In summary, the structure of the central pore, as seen here, was commonly observed on other FIB cross sections of this splat morphology. However, the contact at the splat-substrate interface in other splats was not always as good as in the cross section shown: delamination can sometimes be found under the rim of the splats, as well as, occasionally, porosity. In contrast, cross sections of splashed splats showed coarse grain structures along with NiO phases, and the contact at the interface was usually quite poor. However, cross sections of regular disc-shaped splats showed that over their main flat part, between the central hole and the rim, grains were usually fine, contact between the splat and substrate was good, and as will be shown later, there is evidence of melting of the substrate, but limited oxide is present.

Several TEM cross sections were examined. For example, Fig. 3(a) shows a bright field image of a TEM cross section made across the rim of a disc-shaped splat (see inset SEM image of the entire splat). This splat exhibits an accumulation of NiCr at the periphery (1), topped by a layer of CrO_3 (2), with also some delamination at the splat-substrate interface (3). Furthermore, through EDS elemental mapping (Fig. 3b, c), some chemical intermixing between the splat (Ni) and the substrate (Fe) can be seen (4): melting of the substrate has clearly occurred and it seems that the steel that has melted

has flowed around the molten NiCr, and then gets folded into the splat. Study of this zone via electron diffraction, which allows study of the orientation of the grains, shows that the intermixed zone has a fine grain structure with high angle boundaries (4). EDS linescans across this zone (Fig. 3d) also shows that Fe and Ni interdiffusion across the splat-substrate interface has occurred (5). In contrast, the linescan made across a zone where the splat-substrate interface is clear (Fig. 3e) shows a sharp step-function at the interface.

Study of other TEM cross sections reveals the presence of features such as thin layers of chromium oxide (either Cr_2O_3 or CrO_3) on the outer surface of some splats. NiO is present as a porous phase, not only around the central pores, but also in other pores at the interface or around the rim and splashed zones of splats. Melting of the substrate along with splat-substrate intermixing and diffusion is frequently observed, mostly at the interface in the main flat part of the splat.

3.2 Aluminum Specimen

Observation of the SEM images, following the same method as for the steel specimen, showed that the morphology of the splats found on the aluminum specimen was quite different to the one for the steel specimen. In this case the splats were classified also in the three following categories:

- Thick and almost disc-shaped splats (Fig. 4a), often fragmented or with a large hole in the center where the substrate was bare (~33% of the analyzed series) ($D_m = 28.3$ μm, $20 < D < 43$ μm).
- Very fragmented and thin splats (Fig. 4b), with a circular shape (~49% of the analyzed series) ($D_m = 16.2$ μm, $10 < D < 28$ μm).
- Very irregular splats (Fig. 4c) where it appears that the NiCr liquid has not spread across the substrate surface (~18% of the analyzed series) ($D_m = 17.9$ μm, $10 < D < 25$ μm).

Several FIB cross sections were performed on the different splat types found on the aluminum substrate. One section was made across a very fragmented and thin splat is shown in Fig. 5. It can be seen that the splat thickness increases from the center (1) to the periphery (2). Moreover, from the shape of the grains (2), the NiCr liquid has been ineffective in wetting the surface when impacting on the substrate and has slid away from the point of impact during flattening. Further, almost no material from the splat is found in a large central area (1). The splat-substrate interface is quite porous (3), and the contact between them is poor, and the grain structure irregular and coarse (2). Moreover, in the area marked (4) it appears that there is a part of the splat that suggests fragmentation of the splat droplet under impact. The splat is thin, with an aspect ratio estimated at $\zeta \sim 80$.

This poor contact between the splat and substrate was observed for every splat on the polished aluminum substrate, even for the almost disc-shaped splats. The latter are thicker (ζ is usually around 40, compared to 80 for the splashed ones), with larger grains, but with poor contact. Further, very little oxide can be found even in the center of the splats, which is usually free of NiCr. Finally, no evidence of substrate melting was found.

An example of a TEM cross section is shown in Fig. 6: This TEM cross section was performed across a thick irregular splat. The bright field image (Fig. 6a) shows that the splat-substrate interface is clearly delineated and uniform (1). The contact between splat and substrate is poor: many large pores can be seen at the interface. Elemental mapping (Fig. 6b-f) reveals a layer of chromium oxide on the outer surface of the splat (2). This layer is too thin to get unambiguous electron diffraction data, but it is probably either CrO_3 or Cr_2O_3. There is also a thin layer of oxide on top of the substrate, under the splat, which, on the basis of the EDS maps, is probably Al oxide (3). Furthermore, one can observe a significantly large intermetallic iron-rich particle within the substrate (4). The EDS linescan (Fig. 6g) performed across the splat-substrate interface confirms the absence of any mixing or

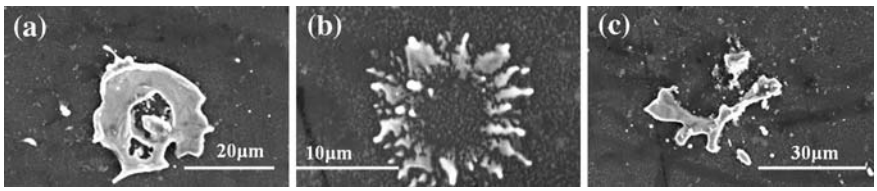

Fig. 4 SEM images of each type of splat found on the aluminum substrate

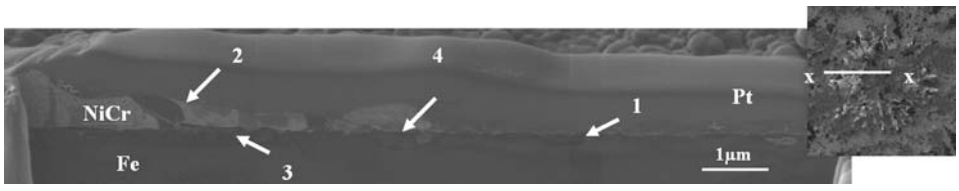

Fig. 5 FIB image of a cross section of a splashed splat found on the aluminum substrate

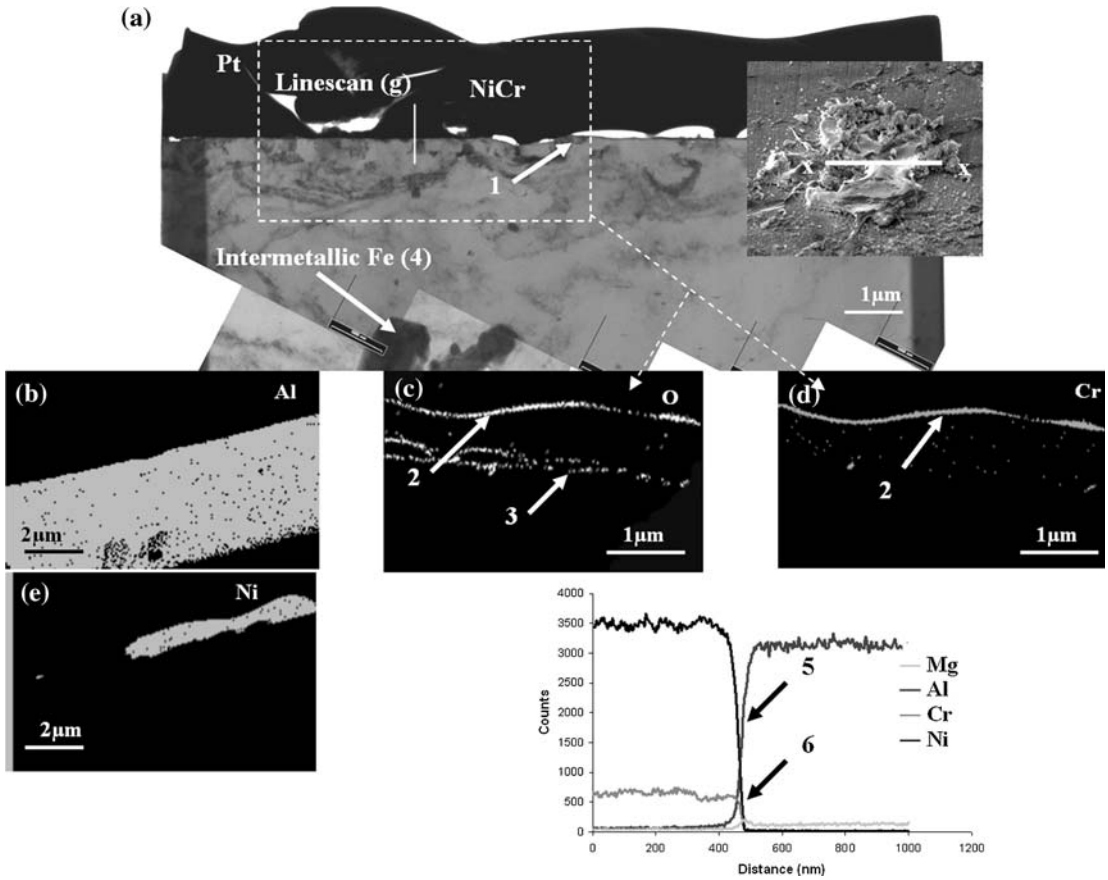

Fig. 6 TEM cross section of an almost disc shaped splat from the aluminum specimen: (a) Bright field image, (b-e) EDS elemental maps, (f) EDS linescan

diffusion between the aluminum and NiCr (5). On the other hand it shows a slightly higher concentration of Mg at the surface of the substrate (6). This was not evident on the mapping due to the lower spatial resolution of the maps. The Mg enrichment is attributable to effects from the heating in air of the substrate and the preferential oxidation of Mg, which segregates this element toward the surface (Ref 6).

On all the TEM cross sections examined on the different types of splats, no sign of chemical mixing between Al and NiCr could be found. The interface was always straight and clear and there were no structural features, such as the formation of additional phases or voids within the substrate. These observations suggest that no melting of the substrate has occurred. Moreover, the contact is mostly very poor with frequent evidence of porosity at the interface. Chromium oxide can be found sometimes either as a thin layer on top of the substrate or as small particle at the interface (in the first case it was probably formed after the flattening of the splat, while in the second case it was probably formed on the periphery of the melted particle before impact), nickel oxide can also be found as large porous clusters, especially on splashy splats. Mapping often reveals the presence of what is assumed to be a thin layer of Al oxide on top of the substrate. It is probably formed during spraying due to the heat of the plasma flame. Finally, intermetallic Fe and Mg-rich phases are frequently observed in the substrate.

4. Discussion

One characteristic of the plasma spraying process is that almost all particles sprayed impact the substrate in a fully molten state. When the NiCr particles impact the stainless steel substrate (see Fig. 7), they heat up the substrate, causing the release of gas such as the chemisorbed water from the surface (Ref 7). This released gas forms one of several pores in the center of the flattened splat, causing a poor contact in this region (Fig. 7-1). The pore may also reach a critical size where it becomes unstable, creating a large bubble-like hole. The presence of oxygen and water-rich gas trapped into this pore(s) is probably responsible for the formation of Ni oxide. This oxide is less stable than both Cr_2O_3 and CrO_3, but its kinetics of formation are faster (Ref 8). Meanwhile, the molten NiCr particle undergoes flattening (Fig. 7-2). It is possible that gas released from the surface is simultaneously covered by the flowing splat and may be pushed at

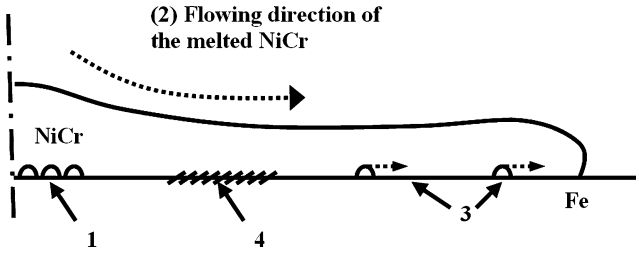

Fig. 7 Schematic representation of demonstrating the process of flowing across a steel substrate

the periphery because of the flow of melted metal (Fig. 7-3). In this situation, good contact between NiCr and the steel substrate can be achieved. The heat from the molten splat is then sufficient to locally melt the steel substrate (modeling showed that temperature at the splat-substrate interface may reach 1660 °C, the melting point of steel being 1454 °C (Ref 9)) (4): the molten steel, pushed by the flowing splat, is then splashed within the splat, as observed by mapping of the interface (Fig. 3b/c). Diffusion across interface between the steel substrate and the splat can also occur in this zone. NiCr and austenitic stainless steel have the same crystal structure and similar lattice parameters, a (both face centered cubic, with lattice parameters of $a = 0.352$ nm for the steel and 0.355 nm for NiCr). Grain growth between the two phases across the interface can therefore take place easily. Electron diffraction studies showed that NiCr and steel grains with the same orientation were found juxtaposed across the interface. Finally, the gas that has been pushed at the rim of the splats is probably the cause of the formation of NiO in this region. Moreover, the delamination under the rim is due to the curl up of the splat, occurring when the splat solidifies and cools down and the upper surface shrinks (Ref 10). The formation of a thin layer of Cr oxide on the outer surface of the splat can be compared to the high temperature oxidation of NiCr alloys (Ref 11). Some Cr oxide may also originate from in-flight oxidation, especially small oxide particles found around the splat-substrate interface (Ref 12).

The formation of the splat on the aluminum specimen is thought to be similar to that observed on the steel substrate in several areas. The gas release from the substrate upon impact and flattening is a key point, probably even more important for this substrate, as it seems that a gas cushion between the flattening splat and the substrate may form (Ref 7). This could explain, on one hand, the porosity that can be found at the interface, and on the other hand, why many splats are very fragmented. That is, it appears as if the NiCr had slid away from the point of impact without adhering to the substrate. Ni and Cr oxides develop in a similar fashion as seen for the steel substrate: NiO can be found in pores, while Cr oxide is present in thin layers on top of some splats.

However, the main difference that has been observed between the splats on the stainless steel specimen and the aluminum specimen is the nature of the splat-substrate interface. Indeed, the contact between the splats and the aluminum substrate is quite poor, and no sign of melting of the substrate, neither mixing or diffusion, has been observed. At first sight, this situation is quite unexpected, as the melting point of aluminum is much lower (649 °C) than for steel (1454 °C). For instance, Li et al. sprayed Mo on several substrates including steel and aluminum and found that melting of the substrate was more likely to occur with an aluminum substrate than with a steel substrate (Ref 13). However, other parameters than the substrate melting point should be taken into account. Firstly, thermal diffusivity is important: at 25 °C, the thermal diffusivity for stainless steel 304L is ~4×10^{-5} and ~58×10^{-5} m^2 s^{-1} for Aluminum 5052 (calculated from (Ref 14)). This means that the heat brought to the substrate by the splat is more likely to be diffused into the bulk substrate for the aluminum, and the temperature at the surface is not elevated as for the steel substrate. Modeling of the splat formation described elsewhere in detail by Tran et al. showed that the thermal diffusivity had a strong influence on the degree of substrate melting (Ref 9).

Another factor is surface chemistry. XPS analysis suggests that compounds such as oxides and hydroxides may be present on both substrates' surface, mainly Fe_2O_3 and FeOOH for steel, Al_2O_3 and AlOOH for aluminum (Ref 7). Upon heating hydroxides get dehydrated and transformed into oxide, which release water vapor. It is also suggested that the oxide/hydroxide layer may be slightly thicker on the aluminum surface (4.2 nm, against 3.5 nm). Surface chemistry and its influence on splat formation is still not well understood, but if there is effectively more hydroxide on the Al specimen, or if it is more prone to release gas upon heating, then the degree of contact between splat and substrate would be compromised, due, for instance, to the presence of an isolating gas cushion, and less heat would be transferred from the splat to the specimen. It is possible then that a combination of those two processes kept the aluminum substrate from reaching its melting point.

Such hypothesis could be studied on one hand using vacuum plasma spraying to spray NiCr on very "clean" Al and steel substrates, in order to limit to the maximum possible extent the influence of surface chemistry, or on the other hand by varying the surface chemistry and comparing splats between specimens made of the same materials. Research focused on investigating these issues is currently underway in a larger study investigating the splat microstructure and splat formation processes as a function of the substrate surface chemistry and roughness.

5. Conclusion

Study of plasma sprayed single splats on aluminum and stainless steel substrates showed that the morphology and the characteristics of the splat-substrate interface were very different from one substrate to another. Splats found on the stainless steel specimen were more regular and disc shaped. But very importantly localized melting of the

substrate and intermixing and diffusion were observed at the interface. Splats on the aluminum substrate were slightly more irregularly shaped. The contact at the splat-substrate interface was usually poor with a lot of porosity. For both type of splats, several oxide phases were observed. Their formation and the formation of the splats were discussed, but further experiments will be needed to fully identify the origins of the differences observed between the steel and the aluminum specimens.

References

1. M. Dorfman, Thermal Spray Basics, *Adv. Mater. Process.*, 2002, p 47-50
2. S. Kitahara and A. Hasui, A Study of the Bonding Mechanism of Sprayed Coatings, *J. Vacuum Sci. Technol.*, 1975, **11**(4), p 747-753
3. V. Pershin, M. Lufitha, S. Chandra, and J. Mostaghimi, Effect of Substrate Temperature on Adhesion Strength of Plasma-Sprayed Nickel Coatings, *J. Therm. Spray Technol.*, 2003, **12**(3), p 370-376
4. H.-D. Steffens, B. Wielage, and J. Drozak, Interface Phenomena and Bonding Mechanism of Thermally-sprayed Metal and Ceramic Composites, *Surf. Coat. Technol.*, 1991, **45**, p 299-308
5. A.T.T. Tran, S. Brossard, M.M. Hyland, and P.R. Munroe, Evidence of Substrate Melting of NiCr Particles on Stainless Steel Substrate by Experimental Observation and Simulations, *Plasma Chem. Plasma Process.*, 2009. doi:10.1007/s11090-009-9192-0
6. C. Lea and C. Molinari, Magnesium Diffusion, Surface Segregation and Oxidation in Al-Mg Alloys, *J. Mater. Sci.*, 1984, p 2336-2352
7. A.T.T. Tran, M.M. Hyland, T. Qiu, B. Withy, and B.J. James, Effects of Surface Chemistry on Splat Formation During Plasma Spraying, of Thermal Spray 2008, *Crossing Borders*, E. Lugscheider, Ed., Pub. DVS-Verlag GmbH, Duesseldorf, Germany, 2008, p 701-706
8. J. Stringer, B.A. Wilcox, and R.I. Jaffee, The High-Temperature Oxidation of Nickel—20 wt% Chromium Alloys Containing Dispersed Oxide Phases, *Oxid. Met.*, 1972, **5**(1), p 11-47
9. A.T.T. Tran and M.M. Hyland, The Role of Substrate Surface Chemistry on Splat Formation During Plasma Spray Deposition by Experiments and Simulations, of Thermal Spray 2009, *Expanding Thermal Spray Performance to New Markets and Applications*, B.R. Marple, M.M. Hyland, Y.-C. Lau, C.-J. Li, R.S. Lima, and G. Montavon, Ed., Pub. ASM International, Materials Park, OH, USA, 2009, p 462-468
10. M. Xue, S. Chandra, and J. Mostaghimi, Investigation of Splat Curling up in Thermal Spray Coatings, *J. Therm. Spray Technol.*, 2006, **15**(4), p 531-536
11. N.S. McIntyre, T.C. Chan, and C. Chen, Characterization of Oxide Structures Formed on Nickel-Chromium Alloy During Low Pressure Oxidation at 500-600 °C, *Oxid. Met.*, 1990, **33**(5/6), p 457-479
12. M. Fukumoto, M. Shiiba, H. Kaji, and T. Yasui, Three-dimensional Transition Map of Flattening Behavior in the Thermal Spray Process, *Pure Appl. Chem.*, 2005, **77**(2), p 429-442
13. L. Li, X.Y. Wang, G. Wei, A. Vaidya, H. Zhang, and S. Sampath, Substrate Melting During Thermal Splat Quenching, *Thin Solid Films*, 2004, **468**, p 113-119
14. MatWeb, *Material Property Data*, 2008 (11/11/2008); Available from: http://www.matweb.com/